# Separation techniques of partial discharges and electrical noise sources: a review of recent progress.

ARDILA-REY, J.A., CERDA-LUNA, M.P., ROZAS-VALDERRAMA, R.A., DE CASTRO, B.A., ANDREOLI, A.L. and MUHAMMAD-SUKKI, F.

2020

# Separation Techniques of Partial Discharges and Electrical Noise Sources: A Review of Recent Progress

**JORGE ALFREDO ARDILA-REY**[1], **(Member, IEEE), MATÍAS PATRICIO CERDA-LUNA**[1],
**RODRIGO ANDRÉS ROZAS-VALDERRAMA**[1],
**BRUNO ALBUQUERQUE DE CASTRO**[2], **(Member, IEEE),**
**ANDRÉ LUIZ ANDREOLI**[2], **(Member, IEEE),**
**AND FIRDAUS MUHAMMAD-SUKKI**[3], **(Member, IEEE)**

[1]Departamento de Ingeniería Eléctrica, Universidad Técnica Federico Santa María, Santiago de Chile 8940000, Chile
[2]Department of Electrical Engineering, Bauru School of Engineering, São Paulo State University (UNESP), Bauru 17033-360, Brazil
[3]School of Engineering, Robert Gordon University, Aberdeen AB10 7GJ, U.K.

Corresponding author: Jorge Alfredo Ardila-Rey (jorge.ardila@usm.cl)

**ABSTRACT** Partial discharge (PD) monitoring is one of the most used tools for diagnosing the condition of electrical equipment and machines that operate normally at high voltage levels. Ideally, PD identification can be easily done if there is a single source acting over the electrical asset during the measurement. However, in industrial environments, it is common to find the presence of multiple sources acting simultaneously, which hinders the identification process, due to sources of greater amplitude hiding the presence of other types of sources of lesser amplitude that could eventually be much more harmful to the insulation system. In this sense, the separation of PD through the use of clustering techniques allows individual source recognition once they have been clearly separated. This article describes the main clustering techniques that have been used over time to separate PD sources and electrical noise. The results obtained by the different authors in the utilization of each technique demonstrates good performance in terms of separation.

**INDEX TERMS** Partial discharges, separation techniques, noise sources, progress, review.

## I. INTRODUCTION

In the modern electrical industry, engineers and specialist technicians are responsible for maintaining and operating the electrical equipment, cables, and machines that integrate the electrical systems of substations or power plants [1]. Extending the useful life of these assets by lessening the sources that may cause deterioration or possible failures is a fundamental part of the work such specialists must perform [1]–[4]. Regarding high voltage electrical assets, it is well known that a big part of the failures usually occurs in the insulation system, due to the uncontrolled presence of multiple ageing mechanisms of electrical, mechanical, thermal, and environmental origin [2], [3], [5]–[7], which, over time,

tend to accelerate the loss of the dielectric properties of the material, leading to the anticipated failure of the equipment.

One of the main indicators when diagnosing the state of insulation in an electrical asset is the online or offline measurement of the activity of partial discharges (PD), since the presence of this phenomenon can be considered a cause and a consequence of most electrical problems in the insulation system [8].

In any electrical equipment, PD activity tends to occur in areas of insulation where dielectric strength is low or where there is a higher concentration of electric field [9]–[11]. In this sense, it is important not to exceed the nominal operating values in order to avoid overstressing and damaging any point or area of the material. However, it has been proven that even operating at nominal voltage levels, PD activity can be detected, and even if it is not producing immediate failure in the equipment, over time it can generate a progressive

The associate editor coordinating the review of this manuscript and approving it for publication was Pavlos I. Lazaridis.

deterioration of the insulation due to the attack of electron-ions and the chemical degradation that occurs in the area [8], [12]–[15].

According to their nature, PD can be classified into three types: internal PD, surface PD and corona PD (see Fig. 1). Internal PD occur within the systems of solid insulation in vacuoles or internal imperfections, surface PD occur on the surface of any insulation under electric field tangential components, and corona PD starts around sharp conductors subjected to high magnitudes of electric field [16], [17]. Some types of PD may be less harmful than others in terms of material degradation, and once identified, they can be easily mitigated during a scheduled maintenance work [18]–[22]. Therefore, it is very important to quantify the PD activity of the equipment during the maintenance process, since it will allow to accurately determine the evolution of any failure or the appearance of new imperfections that may risk the asset operation in the short, medium or long term [15], [23]–[25].

Commonly, PD activity is represented by PRPD (Phase Resolved Partial Discharge) patterns. In this approach, the magnitude and the time of occurrence of the PD pulses are represented, taking as a reference the network voltage (50-60 Hz). For this reason, each type of PD source generates a different PRPD; thus, the identification process can be done through the visual interpretation of these patterns [16], [25]. A correct interpretation of the PRPD will allow the identification of other types of unwanted sources, as is the case of external sources of electrical noise, whose PRPD will depend on the phase correlation of the signals captured (in reference to the network voltage).

For any specialist or intelligent identification system, one of the main constrains of using PRPD for an identification or diagnosis process, is the simultaneous presence of multiple sources of PD or electrical noise, since the patterns obtained under these conditions are difficult to interpret because the sources of greater amplitude hide the presence of other types of sources with less amplitude [21], [22], [26], [27]. Also, many of these omitted sources can become much more damaging to the equipment. For example, internal PD sources detection would reveal problems in the internal structure of the insulation. On the other hand, if the noise levels are very high, it would not be possible to identify other insipient sources of PD that were also associated with some type of serious insulation failure. For this reason, in order to avoid omitting important information associated with the condition of the equipment, it is recommended to carry out a separation process prior to any identification process [22], [28]–[42].

Source separation is carried out mainly through clustering techniques based on the mathematical analysis of the waveform of the acquired pulses, and on the assumption that each type of PD source has a specific behaviour (temporal or spectral). Under these premises, it is possible to extract characteristic parameters from the signals, whether in frequency, time, load, energy, or other variables that allow correct differ-entiation between sources. Subsequently, with this information, two-dimensional or three-dimensional separation maps can be generated, representing the sources through clusters located in different areas of the map, thus generating a clear source differentiation [21], [22], [41], [42]. Once separated, it is easier to obtain the corresponding PRPD to each cluster, so that the individual identification of all the sources can be done.

Although in literature it is possible to find clustering techniques that have proven to be useful when separating different types of PD sources and electrical noise, the obtained results do not always allow optimal separation since there are PD sources and electrical noise whose spectral or temporal content can be similar, and hence the obtained clusters may overlap in the separation map. Additionally, many noise sources that are normally present in industrial environments, such as white noise, can alter the signals associated with PD, affecting some of the mathematical parameters applied by the utilized technique, making it unsuccessful [42]. For this reason, the performance of the separation technique will depend on features such as the type of source being measured, the sensor used in the measurement process, the environment where the measurement is made, and the electrical characteristics of the test object.

This article describes the main clustering techniques implemented in much of the scientific literature focused on the characterization of insulation systems through PD measurement. According to the results presented by the different authors, each technique detailed below has proven to be useful in differentiating multiple sources, even when they act simultaneously. Based on the structure of each technique, an attempt has been made to describe the variables used for the source differentiation in the different separation maps. The subsequent identification process either through PRPD patterns or through intelligent pattern recognition algorithms is beyond the focus of this work and therefore will not be addressed.

## II. TECHNIQUES FOR SOURCE SEPARATION
### A. SEPARATION OF MULTIPLE PD SOURCES USING WAVELET DECOMPOSITION AND PRINCIPAL COMPONENT ANALYSIS

The process of separating PD sources and electrical noise with this technique consists of three stages: an initial wavelet decomposition stage, then a principal component analysis, and finally, the density-based spatial clustering of applications with noise (DBSCAN) that allows the subsequent search and identification of clusters [28]. The wavelet decomposition stage begins by applying the wavelet transform to each acquired PD pulse (original signal). This decomposition process acts as a pair of complementary high-pass and low-pass filters, which decompose the original signal (S) into two new signals, each with half the bandwidth and half the duration of the original signal. As shown in Fig. 2 (a), these new signals are called the approximation (ca) and detail (cd) coefficients.
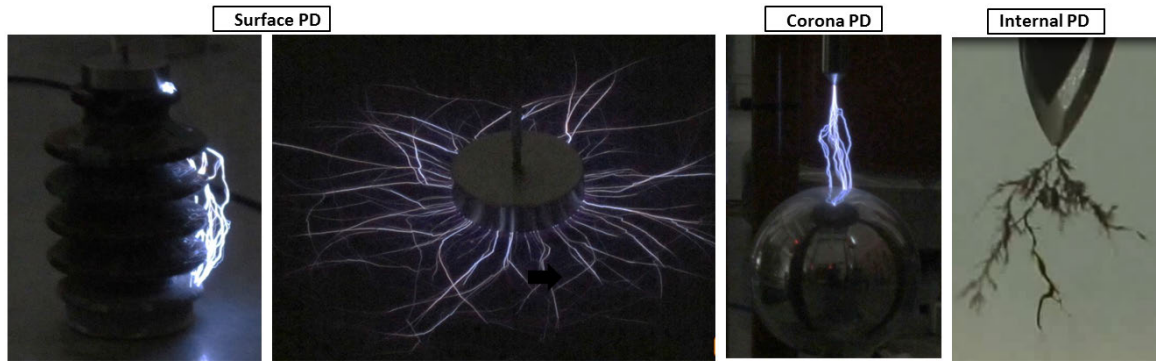
**FIGURE 1.** Effects generated from different PD sources (Images taken experimentally by the co-authors in the high voltage laboratory).
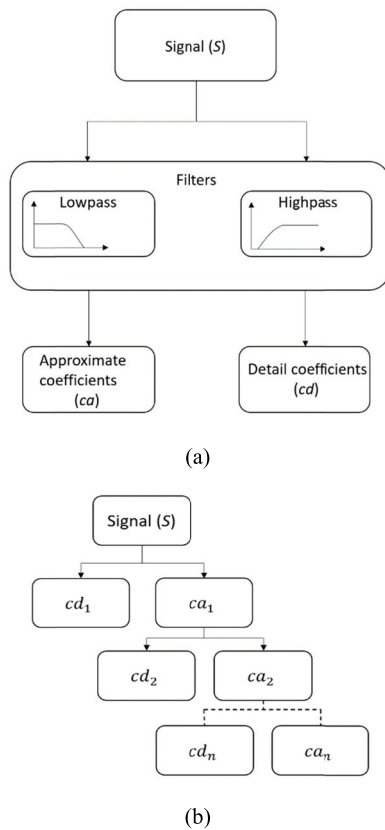


**FIGURE 2.** Representation of the Wavelet decomposition: (a) Action of filters in Wavelet decomposition, (b) Iterative process in wavelet decomposition.

As it is an iterative process, the approximation coefficients are used as the new input for the next level of decomposition and the number of levels can be defined at the beginning of the process.

The above described can be seen in Fig. 2 (b), where the original signal is broken down into a certain number of levels and each level contains a signal with half the bandwidth and half the number of samples in the time domain of the signal from the previous level. Once this filtering process

is completed, the original signal is represented as a series of scaled and displaced transformations in relation to the mother wavelet (reference function). Therefore, the coefficients obtained represent a degree of correlation between the original signal and the mother wavelet [28], [43], [44]. In this technique, the 9th order ''Symlet'' family was used as the mother wavelet since, for this particular case, this mother wavelet allowed the successful decomposition for PD signals [28], [45]. However, different methodologies can be found in literature, that allow the optimal selection of the Mother Wavelet that best adjusts to the temporal characteristics of each signal according to the acquisition system that is being used. Among these methodologies we can find: CBWS (correlation based wavelet selection), EBWS (energy based wavelet selection), SNRBWS (signal-to-noise-ratio based wavelet selection), SWTBWS (stationary wavelet transform based wavelet selection) and NewEBWS (new energy based wavelet selection) [46], [47].

Then, for the separation process, the distribution of signal energy in each decomposition level is used, as indicated in (1) and (2):

$$E_{D_i} = \frac{\sum_{j=1}^{N_{ci}} Cd_{i_j}^2(t)}{\sum_{i=1}^{n} \sum_{j=1}^{N_{ci}} Cd_{i_j}^2(t) + \sum_{j=1}^{N_{cn}} Ca_n^2(t)} \cdot 100 \quad (1)$$

$$E_{A_n} = \frac{\sum_{j=1}^{N_{cn}} Ca_n^2(t)}{\sum_{i=1}^{n} \sum_{j=1}^{N_{ci}} Cd_{i_j}^2(t) + \sum_{j=1}^{N_{ci}} Ca_n^2(t)} \cdot 100 \quad (2)$$

where $E_{Di}$, represents the energy for the levels of detail and $E_{An}$ the energy for the levels of approximation. These energy levels are more effective in representing the PD pulses than the wavelet coefficients themselves, in terms of dimensionality reduction and elimination of the influence of pulse polarity. Finally, principal component analysis (PCA) was used to implement the clustering and separation process of each source. PCA is a widely used method for reducing data dimension [28], [48]–[50]. In this case, the PCA is applied to reduce to three parameters the number of energy levels associated with the different levels of decomposition, thus allowing the representation of the PD signals on a 3D classification

map through clusters, where the grouping or selection of the clusters is done by the authors through DBSCAN [20], [51], [52]. DBSCAN only contributes to the partitioning or automatic search of clusters from the n points that make up the separation map.

As described in [28], the performance of the clustering technique was validated in different test objects such as induction motors, synchronous generators and distribution cables. In [53], the clustering technique was also applied to PD sources in medium voltage cables, but using t-Distributed Stochastic Neighbor Embedding (t-SNE) as a method of dimensional reduction and Simple Statics-based Near Neighbor SSNN) for the clusters' search and selection. As described by the authors, with these new changes in the structure of the technique, there was an improvement in the speed and identification rate of the sources.

### B. SEPARATION OF PD SOURCES TROUGH T-F MAPS

To address the problem of separating PD signals and electrical noise with this clustering technique, one of the main considerations is to assume that PD pulses associated with the same type of source present a similar temporal and spectral behaviour [21], [22], [54]–[57]. In this sense, the technique is based on the transformation of the time series of the obtained pulses (which can be from PD or electrical noise), into time sub-series, corresponding to pulses with a similar waveform. To carry out this procedure, the equivalent duration of the waveform and the equivalent bandwidth of the spectrum in each pulse are represented on a two-dimensional map called the Time-Frequency (TF) map [21].

In order to perform a correct extraction of the most important characteristics associated with each type of source it is necessary that the variables used for the generation of the clusters in the separation map have a clear independence regarding the amplitude of the signals, this will avoid that the obtained clusters present, in some cases, a high dispersion with respect to their centroids [29]. In accordance with the above, in this technique the pulses of the acquired $S(t)$ signals are first normalized (3), later, the standard deviation of the normalized signal for the time and frequency domain is obtained, see (4) and (5) [29].

$$\tilde{s}(t) = \frac{s(t)}{\sqrt{\int_o^T s(t)^2 dt}} \tag{3}$$

$$\sigma_T = \sqrt{\int_0^T (t - t_0)^2 \tilde{s}(t)^2 dt} \tag{4}$$

$$\sigma_F = \sqrt{\int_0^\infty f^2 \left| \tilde{S}(f) \right|^2 df} \tag{5}$$

where, $f$ represents the frequency, $\tilde{S}(f)$ the Fast Fourier Transform (FFT) of $\tilde{s}(t)$, and $t_0$ corresponds to the "gravity centre" of the normalized signal and is defined by (6).
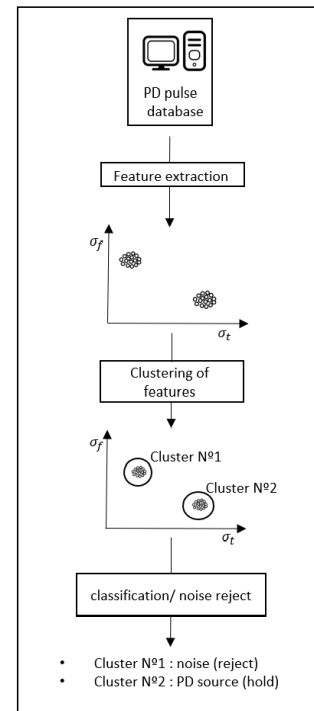
$$t_0 = \int_0^T t\tilde{S}(t)^2 dt \tag{6}$$



**FIGURE 3.** Diagram of the separation process with TF maps.

In this way, the pulses are represented in the separation map through two parameters $\sigma_T$ and $\sigma_F$, which are used for the formation of the different clusters associated with each source found, see Fig. 3. In [54] the use of Fuzzy Maximum Likelihood (FML) is mentioned, for the cluster selection process on the separation map.

After the clustering process is complete, subsequent identification can be more easily performed on each cluster by visual evaluation of PRPD patterns or by applying intelligent pattern recognition techniques such as those described in [22], [54], [57]. Although some studies have shown that the performance of this technique can be influenced by parameters such as noise level, sampling frequency, acquisition time, number of samples and vertical resolution of the measurement system [58], the results obtained so far indicate that the technique shows a very good performance in separating multiple sources of PD and electrical noise. TF maps are currently part of commercial PD measurement systems.

### C. SEPARATION OF PD SOURCES BY THE CHARACTERIZATION OF PULSES WAVEFORM

This technique is based on the extraction of characteristic parameters taken from the temporal and spectral behaviour of the signals obtained [30], [31]. Commonly, there are two main factors that can help differentiate types of PD sources, these factors are associated with the physical characteristics that cause the PD pulses and the paths the signals travel to get to the measurement point, where the sensor is located [10]. Under these premises, and based on the experimental
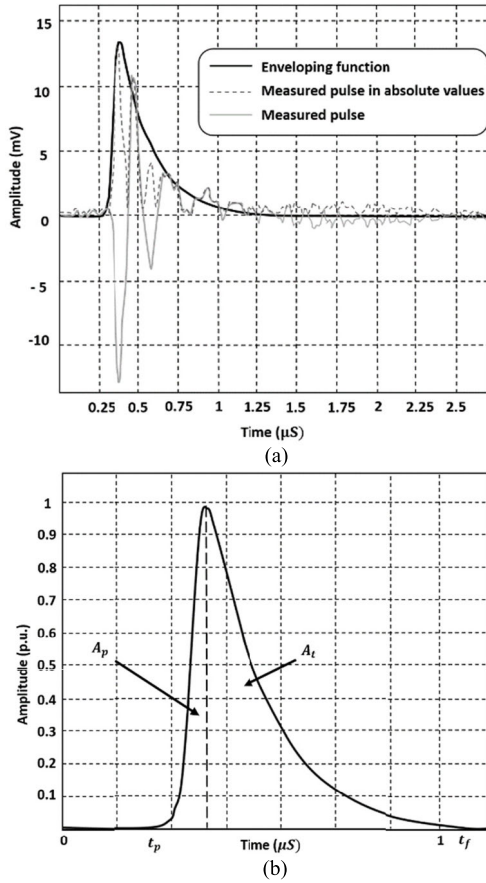
**FIGURE 4.** Envelope function and parameters of the technique. (a) PD pulse with respective envelope function, (b) Ap and At areas of the envelope function.

results obtained by the authors of this technique, it has been possible to show that the pulses associated with the same type of source show certain similarities in the frequency spectrum and in the nature of the envelope function that adjusts to each type of signal, see Fig. 4 (a).

In summary, the authors propose a mathematical model that allows us to accurately characterize the waveform of a pulse through a damped mathematical function $f(t)$ (7). $f(t)$ is going to be composed of two other functions, $g(t)$ that corresponds to a sinusoidal function (8) and $h(t)$, the modulating and enveloping function that is named asymmetric hyperbolic secant (AHS) (9).

$$f(t) = g(t) \cdot h(t) \tag{7}$$
$$g(t) = sen(wt - \varphi) \tag{8}$$
$$h(t) = \frac{I_0}{e^{\alpha(t - t_0)} + e^{\beta(t - t_0)}} \tag{9}$$

The functions $g(t)$ and $h(t)$ are defined based on six different parameters, that is: $\alpha$, $\beta$, $I_0$, $t_0$, $f$ and $\varphi$. Where $g(t)$ is a function of the frequency ($f = w/2\pi$), and its phase shift angle $\varphi$. The parameter $t_0$ in (9) represents the time shift of $h(t)$ and $I_0$ characterizes the amplitude of $h(t)$. The value of $I_0$ is related to the peak value ($I_p$) of the PD pulse according

to (10). Finally, (11) defines the time the maximum peak is reached [31]:

$$I_p = \frac{I_0 \cdot \beta}{\alpha + \beta} \cdot \left(\frac{\alpha}{\beta}\right)^{\frac{\alpha}{(\alpha + \beta)}} \tag{10}$$
$$t_p = \frac{\ln(\beta/\alpha)}{\alpha + \beta} \tag{11}$$

By adjusting the values of $\alpha$, $\beta$, $I_0$ and $t_0$, it is possible to identify the most suitable envelope function to modulate the sine wave. These values are obtained through least squares, searching for the best correspondence between the original signal and $f(t)$. Since the values of $\alpha$ and $\beta$ depend on the magnitude of the discharge, for the clustering process it is necessary to identify other parameters that have a greater relationship with the pulse waveform. In order to achieve this, the envelope curve or modulating function is divided by the value of $I_p$, thus obtaining the magnitude in values per unit. Based on the above, two parameters are obtained that correspond to the $A_p$ and $A_t$ areas, which are generated below the envelope function and can be differentiated from the maximum value of the same function, see (12) and (13):

$$A_p = \int_0^{t_p} \frac{h(t)}{I_p} dt \tag{12}$$
$$A_t = \int_{t_p}^{t_f} \frac{h(t)}{I_p} dt \tag{13}$$

As seen in Fig. 4(b), the left area of the envelope is defined as $A_p$ and the area on the right side as $A_t$. Finally, the frequency $f$, which is another parameter used in this technique to perform source separation, is determined by analyzing the frequency spectrum $F(f)$ of the PD signals. Basically, $f$ corresponds to the arithmetic mean of the values in an interval $[f_1, f_2]$ where the energy of the spectrum is more significant, that is, the frequency band that has spectral components greater than 70%, see (14) [30], [31].

$$f = \frac{\int_{f_1}^{f_2} f \cdot F(f) \cdot df}{\int_{f_1}^{f_2} F(f) \cdot df} \tag{14}$$

This way, by extracting the parameters $A_p$ and $A_t$, and $f$ from a group of signals and representing them on a two or three-dimensional separation map, it is possible to achieve a visual separation of the PD sources. One of the advantages in the applied methodology is that the mathematical model allows to reconstruct the PD pulses with reasonable accuracy. Furthermore, as reported in [30], the required computational capacity is lower when compared to other separation techniques. It is worth mentioning that, for this technique, the noise sources are previously removed through the use of a wavelet filter. Furthermore, the authors do not report the use of cluster search methods in separation maps.

### D. PD SOURCE SEPARATION BY $I_{PEAK}$ QE CLUSTERS TECHNIQUE

As indicated in [32], this clustering technique called "$I_{peak}QE$ cluster technique" is based on the use of the values

of load ($Q$), energy ($E_k$) and the peak amplitude ($I_{peak}$) of the PD pulses, to carry out the source separation process through two-dimensional separation maps ($I_{peak}$ vs $Q$, $I_{peak}$ vs $E_k$ and $Q$ vs $E_k$). The experimental results showed that these parameters allow an adequate separation as long as the pulses waveform has a different temporal behaviour for each type of source. On the other hand, it was found that the $E_k/I_{peak}$, $I_{peak}/Q$ y $E_k/Q$, relationships can also be used as separation parameters, being more sensitive to subtle differences in the waveform of the signals associated with each source.

Likewise, the authors indicated that the use of these parameters allows obtaining a more robust separation in the face of variations in the parameters of the acquisition system used, such as the sampling frequency, the period, the number of samples and the vertical resolution of the signals captured, which is useful in the case of using acquisition systems with different characteristics in the same asset, since the results obtained in terms of clustering and separation would be similar.

According to the structure of the technique, to obtain the $I_{peak}$ value, the signal of the PD pulse is recorded in a vector $y_k$, and $I_{peak}$ value is obtained from the maximum value of $y_k$. Next, the apparent charge value of the PD pulse ($Q$) is obtained in the time domain (taking $Q$ as the integral over the time of the duration of the PD pulse ($y_k$)). However, due to the implemented measurement circuit, the load value may not be appropriate according to its definition, since the PD pulses can present oscillations that affect the actual load value. To soften the effect of these oscillations, the $y_k$ signal is filtered by a second-order Butterworth low-pass filter, thus reducing possible calculation errors. Using the filtered signal $x_k$, the indices $i_a$ and $i_b$, are obtained, which represent the first zero crossings of the peak current value (see Fig. 5(a)). Then, as shown in (15), the load is obtained as an approximation of the integral of the first peak value of $x_k$ between the values of $i_a$ and $i_b$, where, $dT = 1/Fs$, and $Fs$ is the sampling frequency of the acquisition system.

$$Q = dT \sum_{i=i_a}^{i_b} x_k(i) \qquad (15)$$

Finally, the calculation of the energy $E_k$ is obtained from the voltage signal $v_k$ as shown in (16)

$$E_k = \frac{dT}{R \cdot N} \cdot \sum_{i=f_1}^{f_2} S_k(i) \qquad (16)$$

where $R$ is the input impedance of the acquisition system, $N$ represents the number of samples, and $S_k$ is the FFT of $v_k$. $S_k$ is obtained by limiting the spectrum in frequency, considering the frequency components greater than 10% of the maximum peak of the spectrum, that is, the frequency spectrum between $f_1$ and $f_2$ according to Fig. 5(b). This truncation is carried out to avoid that the spectral components associated with electrical noise cause errors in the energy calculation [32]. For this separation technique, the use of automatic search methods or selection of clusters is not reported either.
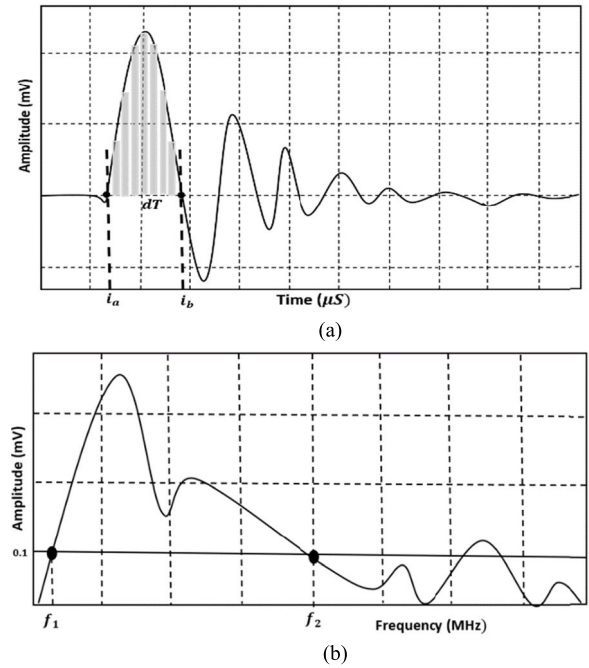


**FIGURE 5.** Parameters of truncation necessary to applied in this technique: (a) Indices $i_a$ and $i_b$ of the filtered signal $x_k$, (b) Truncation of the frequency spectrum for the calculation of $E$ k between $f_1$ and $f_2$.
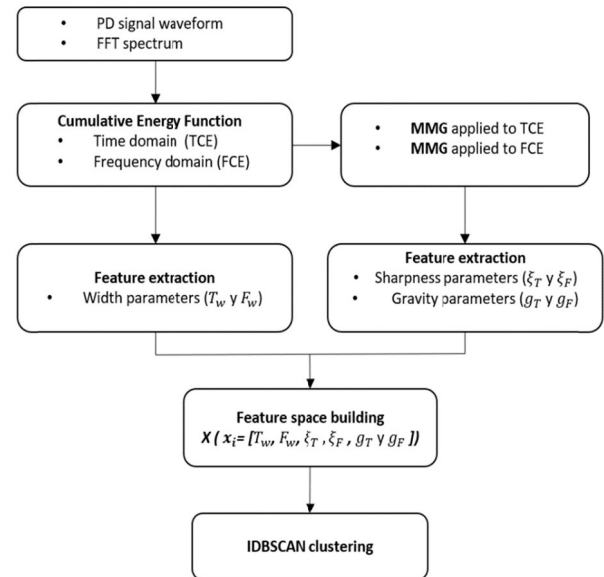


**FIGURE 6.** Flowchart of the separation algorithm using MMG and CE technique [33].

### E. SOURCE SEPARATION USING CUMULATIVE ENERGY FUNCTION AND MATHEMATICAL MORPHOLOGY GRADIENT

In [33], a new algorithm for the separation of PD signals is presented, based on the application of the cumulative energy function (CE) and the Mathematical Morphological Gradient (MMG) to the PD pulses and electrical noise captured during the measurement process. According to this technique, three

pairs of characteristic parameters (width, sharpness and gravity) are extracted from the CE and the MMG, both in the time domain and in the frequency domain. This way it is possible to compose a space with six-dimensional characteristics ($T_w$, $F_W$, $\xi_T$, $\xi_F$, $g_T$ and $g_F$). For the separation procedure, two-dimensional separation maps are generated from the $T_w$ - $F_W$, $\xi_T$ - $\xi_F$ and $g_T$ - $g_F$ combinations. Depending on the test object and conditions, one of these three charts may have a better result during separation. Fig. 6 shows the algorithm that summarizes the procedure used in this technique. This algorithm uses the waveform of the acquired PD signal and the calculated frequency spectrum to obtain the energy functions accumulated in time (TCE, $ET(t_k)$) and in the domain of the frequency (FCE, $EF(f_k)$); functions defined in (17) and (18).

$$E_T(t_k) = \frac{\sum_{i=1}^{k} v(t_i)^2}{\sum_{i=1}^{N} v(t_i)^2} * 100 \quad k = 1, \ldots, N \quad (17)$$

$$E_F(f_k) = \frac{\sum_{i=1}^{k} F(f_i)^2}{\sum_{i=1}^{N/2} F(f_i)^2} * 100 \quad k = 1, \ldots, \frac{N}{2} \quad (18)$$

$E_T(t_k)$ represents the energy accumulated in the time domain up to the instant $t_k$, $E_F(f_k)$ is the energy accumulated in the frequency domain up to the frequency $f_k$, $v(t_i)$ is the signal sampled at the instant $t_i$, $F(f_i)$ is the amplitude at the frequency $f_i$ obtained through the FFT, and $N$ is the total number of samples. Regarding these energy functions, the parameters of width $T_w$ and $F_W$, are defined in (19) and (20) and describe the time duration and the frequency bandwidth of PD signal.

$$T_w = t|_{E_t=80} - t|_{E_t=20} \quad (19)$$
$$F_w = f|_{E_f=80} \quad (20)$$

The next step is the calculation of the MMG defined in (21) and, as can be seen, makes use of the energy functions ($E_T(t_k)$ or $E_F(f_k)$) and g, (a parameter defined as an element of structure) [33].

$$mg(n) = E \oplus g(n) - Eg(n) \quad (21)$$

The MMG is used to characterize the increasing inclination of TCE and FCE. To achieve this characterization, (22) and (23) are defined, where $\xi_T$ and $\xi_F$, are the maximum values obtained from $mg_T$ and $mg_F$, that correspond to the sharpness parameters.

$$\xi_T = \max\{mg_T\} \quad (22)$$
$$\xi_F = \max\{mg_F\} \quad (23)$$

Subsequently, the gravity parameters are obtained using MMG according to (24) and (25), which represent the instant ($g_T$) and the frequency ($g_F$) where the MMG is greater.

$$g_T = \frac{\sum_i (t_i * mg_{Ti})}{\sum_i mg_{Ti}} \quad (24)$$

$$g_F = \frac{\sum_i (f_i * mg_{Fi})}{\sum_i mg_{Fi}} \quad (25)$$

This is how the six-dimension feature space is composed. Then, the separation maps described above are generated

using the time and frequency combinations of the characteristic parameters, that is, $T_w$ - $F_W$, $\xi_T$ - $\xi_F$ and $g_T$ - $g_F$. Finally, DBSCAN is used in the generated maps to automatically search for clusters.

Although the presented method uses a space of six characteristics, in [34] the same authors propose an improvement and reduce the space to only four dimensions ($T_w$, $F_W$, $\xi_T$ and $\xi_F$), further redefining the method for the calculation of these values. In addition to this change, and in order to achieve greater efficiency, a separation quality evaluation parameter called $J_T$, based on the density function [59] is used. Finally, in [35] a new variation of the technique is presented, incorporating an algorithm that optimizes the parameters obtained from the CE function and redefining $J_T$, hence maximizing the separation power of the method, and an adequate separation is obtained for three or more simultaneous sources according to reports from the authors. For this technique, the search for clusters in the separation map is done through DBSCAN or FML (fuzzy maximum likelihood) depending on the number of data. DBSCAN is applied to large databases, while FML is adopted for databases with less than 1000 samples [34].

### F. PD AND ELECTRIC NOISE SOURCE SEPARATION USING S TRANSFORM AND BAG OF WORDS

With this technique, once the measurement process has been completed, each of the obtained signals is normalized, thus compensating for the variability that exists in the amplitude of the data acquired [36]. Next, the time-frequency S transform (ST) is applied to the normalized signals in order to obtain an information matrix that incorporates the temporal and spectral characteristics of each signal. Equation (26) shows how this time-frequency representation is obtained from a PD pulse or electrical noise:

$$A(\tau, f) = \left| \int_{-\infty}^{+\infty} x_n(t) \frac{|f|}{\sqrt{2\pi}} e^{-\frac{(t-\tau)f^2}{2}} e^{-j2\pi ft} dt \right| \quad (26)$$

where $\tau$ is a parameter representing the location over the timeline and $x_n$ is the normalized pulse.

Once the ST-amplitude matrix is obtained, it is converted into a grayscale image through (27):

$$s_{ij} = \frac{a_{ij} - min(a_{ij})}{max(a_{ij}) - min(a_{ij})} \quad (27)$$

where, $a_{ij}$ represents one of the elements that are part of the matrix and $s_{ij}$ is an element of the image. This transformation to an image of the information matrix is carried out to extract the most important characteristics associated with a segment of the image, where the most relevant values in terms of information (non-zero value) are concentrated. According to the methodology of this technique, the extraction is done through the Bag of Words (BoW) method, which is normally applied to the field of image retrieval and image classification from the natural language processing.

With the application of the BoW method, the image was converted into a "feature descriptor" vector, which has a
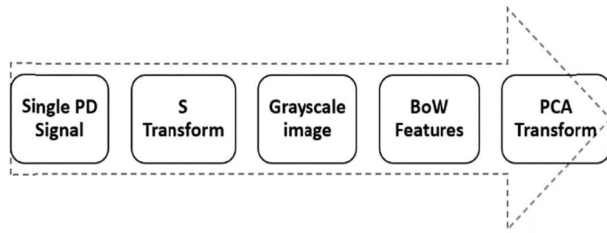
**FIGURE 7.** Sequence for the feature extraction from PD signals.

specific length depending on the pulses obtained. Although the reduction of information with this method is significant, it was necessary to apply PCA in order to reduce the dimensionality of the data. Finally, each pulse is represented by four characteristic parameters, which are used to generate the clusters on a two-dimensional separation map. Once the clusters are generated in the separation map, they are selected with the unsupervised cluster search model named Gaussian mixture model (GMM). Fig.7 summarizes the procedure applied with this technique.

According to the results obtained by the authors of this technique, it was possible to differentiate up to four types of PD sources acting simultaneously. For the clusters generation in the separation maps, out of the four obtained with PCA, only the first two main components were used.

### G. SOURCE SEPARATION USING LINEAR PREDICTION ANALYSIS AND ISOLATION FOREST ALGORITHM

In [37], a clustering technique that uses linear prediction analysis (LPA) and isolation forest algorithm (IFA) is presented to separate different sources acting simultaneously during a measurement process, into clusters. By using LPA, it is possible to extract the most representative characteristics from the waveforms of the PD pulses. This procedure establishes a twelve-dimensional feature space, which is subsequently reduced to two dimensions using PCA. With these two parameters and a third parameter obtained from the IFA, a three-dimensional separation map is established. Generally speaking, the LPA is based on the fact that the value of a sample at the present time can be approximated by a linear combination of several values of past samples. This way it is possible to obtain a linear prediction cepstrum coefficient (LPCC), if the quadratic sum of the difference between the real value and the linear prediction reaches a minimum value.

According to the established procedure for this technique, PD signals can be considered as the outputs of a system. This way, the relationship in the time domain between an input signal and an output signal can be described as a linear constant coefficient difference equation, and is expressed as indicated in (28).

$$x(n) = \sum_{i=1}^{p} a_i x(n-i) + G \sum_{l=1}^{q} b_l u(n-l) \quad (28)$$

where, $x'(n)$ is the input of the system and $x(n)$ is the output; $a_i$, $b_i$ and $G$ are parameters of the PD system, likewise, $p$

and $q$ represent the order of the system. A very important consideration is that, in order to simplify the system and avoid solving a nonlinear equation, the parameters $b_l$ are set to 0, therefore (28) is represented as follows:

$$x'(n) = \sum_{m=1}^{p} a_m x(n-m) \quad (29)$$

where $x'(n)$ is the estimated value of $x(n)$, which is obtained from $p$ past values and where $a_m$ is the linear prediction coefficient (LPC). This system cannot estimate the current signal exactly, and consequently it has an error, defined in (30), as the difference between the signal value $x(n)$ and the estimated value of $x'(n)$:

$$e(n) = x(n) - x'(n) = x(n) - \sum_{i=1}^{p} a_i x(n-i) \quad (30)$$

Then, the quadratic error is given by:

$$E(n) = \sum_n e^2(n) = \sum_n \left[ x(n) - \sum_{i=1}^{p} a_i x(n-i) \right]^2 \quad (31)$$

The LPC $a_i$ is determined by minimizing the value of $E(n)$ and with the partial derivative of LPC equal to 0.

$$\frac{\partial E}{\partial a_j} = 2 \sum_n x(n) x(n-j) - 2 \sum_{i=1}^{p} a_i \sum_n x(n-i)$$
$$x(n-j) = 0 \quad (32)$$

Finally, the LPCC is obtained by the recursive formula (33).

$$L(1) = a_1,$$
$$L(n) = a_n + \sum_{i=1}^{n-1} \left( 1 - \frac{i}{n} \right) a_i h(n-i),$$
$$2 \leq n \leq p \quad (33)$$

where $L(n)$ refers to the LPCC, which can be calculated from the LPC value. As indicated initially, the order of LPA is twelve, which means that a twelve character dimensional space is established after the extraction of LPCC features. The dimensionality of the feature space is then reduced to two by applying PCA [37], [60]. Finally, the IFA anomaly detection algorithm is used in order to quantify the clustering degree of the signals from the data obtained with PCA. This allows obtaining a third characteristic parameter called height score. This way the clustering technique will allow obtaining a three-dimensional separation map. To search and select the clusters, the authors use the Fuzzy C-means (FCM) method (the grouping is done from a centroid that is updated iteratively until it converges to the best value). In accordance to the results obtained with this technique, the authors managed to separate up to three PD sources acting simultaneously.

### H. SEPARATION OF PD SOURCES AND ELECTRICAL NOISE THROUGH THE CHROMATIC TECHNIQUE

This technique was first applied to PD analysis in [38]. According to its structure, each type of PD source has a different colour signature, which can be represented from three specific parameters, each of these parameters is derived from

colour science where an RGB (red, green and blue) colour space is transformed to an HLS space ("hue", "lightness" and "saturation") [38, 39]. In this sense, $H$ is related to the average frequency or characteristic angular frequency ($W_c$), $L$ is the signal energy content ($E_b$), and $S$ is the Equivalent signal bandwidth ($B$). (34), (35) and (36) define the parameters $W_c$, $E_b$, and $B$ [39], [40].

$$\omega_c = \frac{\int \omega \, |F(\omega)|^2 \, d\omega}{2\pi E_b} \qquad (34)$$

$$E_b = \int |f(t)|^2 \, dt = \frac{1}{2\pi} \int |F(\omega)|^2 \, d\omega \qquad (35)$$

$$B = \sqrt{\frac{1}{E_b} \int (\omega - \omega_c)^2 \, |F(\omega)|^2 \, d\omega} \qquad (36)$$

where $F(w)$ is the FFT of $f(t)$, $f(t)$ corresponds to the pulse of a partial discharge in time, and $w$ is the angular frequency. In [39], these three parameters were used to obtain a 3D separation map where it was possible to adequately classify different UHF (Ultra high frequency) sources of PD and electromagnetic noise captured with an antenna, while discharges acting simultaneously on various test objects. Likewise, it was found that the clusters associated with each type of source were located in different positions on the separation map, which is adequate when there are simultaneous sources during the measurement. This same technique was also used later in [40], in order to separate PD sources and electrical noise obtained from three different inductive sensors (a high-frequency current transformer, an inductive loop sensor, and a Rogowski coil). The results showed that separation with lower frequency signals from inductive sensors (up to 100 MHz) was also possible, managing to separate up to three different sources. Additionally, it was evidenced that the $W_c$ and $B$ parameters were the most sensitive when differentiating PD types and electrical noise [40]. The use of cluster search methods was not reported for this technique.

### I. SPECTRAL POWER CLUSTERING TECHNIQUE (SPCT)

This technique of clustering PD sources and electrical noise was first proposed in [41], [42]. According to the description of the technique, FFT $S(f)$ is applied to each of the PD $S(t)$ pulses obtained during the measurement process, making it possible to select two frequency bands called Power Ratio Low (PRL) and a Power Ratio High (PRH), which include the high and low spectral power of greatest interest in the signal. As observed in (37) and (38), both frequency bands are delimited by two separation intervals $[f_{1l}, f_{2l}]$ for PRL and $[f_{1h}, f_{2h}]$ for PRH.

$$PRL = \frac{\sum_{f_{1l}}^{f_{2l}} |s(f)|^2}{\sum_0^{f_t} |s(f)|^2} \qquad (37)$$

$$PRH = \frac{\sum_{f_{1h}}^{f_{2h}} |s(f)|^2}{\sum_0^{f_t} |s(f)|^2} \qquad (38)$$

The parameters $f_{1l}, f_{2l}, f_{1h}, f_{2h}$, that are part of both separation intervals, and $f_t$ that correspond to the maximum spectral con-

tent of each signal, can be adjusted either manually or automatically. Likewise, to guarantee the correct application of the technique, it is necessary to comply with some restrictions: $(0 \le f_{1l} < f_{2l})$, $(f_{1h} < f_{2h} \le f_t)$ and $(f_{1l} < f_{2h})$. Finally, with the values of PRL and PRH, a two-dimensional separation map called PR (Power Ratio) map is established and the clusters associated with each source are formed. As indicated in [61]–[64] k-means was used to search for groups on PR maps. The results obtained with this technique show that up to four different sources of PD and electrical noise can be separated, even if they are simultaneously acting [62]. Fig.8 summarizes the clusterization process with this technique.

The SPCT was initially presented as a manual clustering technique where the separation intervals had to be adjusted manually, based on the spectral content of the signals being acquired. In [61], [62], it was shown that manual interval selection did not always allow obtaining the best separation between sources; even if the separation intervals were correctly selected by the system operator, the clusters associated with different sources could overlap on the separation map, limiting any diagnosis. For this reason, an automatic interval selection algorithm based on the dispersion of the spectral power of the acquired pulses was implemented [61]. This algorithm allowed to automatically identify the frequency bands where the sources presented a clear separation.

Subsequent works evaluated the application of different optimization techniques such as: particle swarm optimization [63], [65], genetic algorithms [66], hill climbing [63], [64] and differential evolution [64]. The results confirmed better separation than that obtained manually and with the automatic selection algorithm.

A complement to the SPCT technique was presented in [67], using a third parameter to obtain a three-dimensional separation map. In this case, UHF PD and electromagnetic noise signals captured from antennas were used. The parameter used for the third axis of the separation map corresponds to the effective pulse duration time, which provides relevant information associated with the temporal behaviour of the signals. In (39) this parameter is mathematically defined.

$$t_{eff} = \frac{\int_0^T \tilde{s}(t)^2 \, dt}{\tilde{s}(t)^2_{max}} = \frac{1}{\tilde{s}(t)^2_{max}} \qquad (39)$$

where $\tilde{s}(t)$ corresponds to the normalized pulse $s(t)$ and $s(t)max$ represents the maximum value of the signal.

### III. DISCUSSION AND CONCLUSION

This work presents an exhaustive summary of the main clustering techniques used in the separation processes of PD sources and electrical noise. These techniques' theoretical description and mathematical procedures are discussed in detail, as well as the utilized references, which were carefully selected in order to facilitate the analysis of the tests and experimental results obtained by the different authors for any reader.
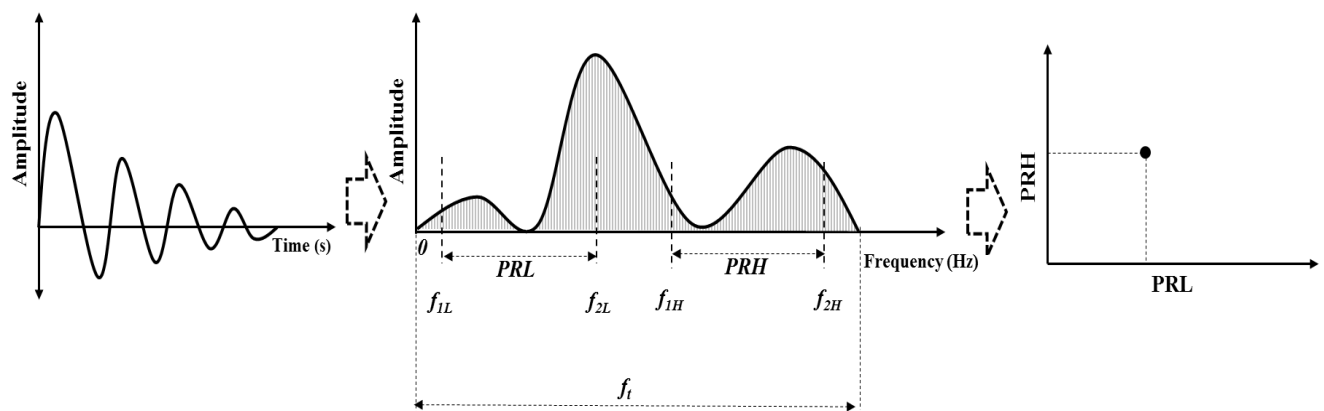
**FIGURE 8.** Spectral-power clustering technique application process.

**TABLE 1.** Main characteristics of the analyzed clustering techniques.

| Techniques | Dimensionality of the separation map | Parameters used | Additional processing |
|---|---|---|---|
| Based on wavelet and PCA | 3D | Energy for $E_D$ detail levels and energy for $E_{A_n}$ approach levels. | Dimensionality reduction through PCA or t-SNE. |
| T-F maps | 2D | Standard deviation of the normalized signal for the time domain $\sigma_T$ and the frequency $\sigma_F$ | --- |
| Characterization of pulses waveform | 2D o 3D | $A_p$, $A_t$, and $f$ are parameters obtained from the envelope and the signal spectral behaviour. | Only at the beginning of the process, applying a wavelet filter to eliminate noise. |
| $I_{peak}QE$ clusters | 2D | $I_{peak}$, $Q$, and $E_k$, parameters, obtained from the temporal and spectral behaviour of the signal | The application of a Butterworth filter is necessary to obtain a more precise value of the apparent charge of the pulses. |
| Based on CE and MMG | 2D | Width ($T_w$, $F_W$), sharpness ($\xi_T$, $\xi_F$), and gravity ($g_T$, $g_F$) | It was necessary to establish $J_T$ and an algorithm that optimizes the CE function in order to improve the results in terms of separation from the initial technique. |
| Based on S transform and bag of words | 2D | "Feature descriptor" vector that incorporates the temporal and spectral characteristics of the signals | PCA is necessary in order to reduce the variables obtained in the characteristics vector. |
| Based on LPA and IFA | 3D | LPCC feature extraction (12-dimensional feature) and the height score obtained from the IFA | PCA is applied in order to reduce the feature space to two dimensions. |
| Chromatic Technique | 3D o2D | $W_c$, $E_b$, y $B$ | --- |
| SPCT | 2D | PRL and PRH | To improve the results of the source separation it is necessary to apply optimization algorithms or automatic identification to obtain the best values $f_{1l}$, $f_{2l}$, $f_{1h}$, $f_{2h}$, and $f_t$. |

As evidenced in this article, one of the main advantages of applying any of these methodologies, prior to the identification process, is to effectively individualize or differentiate the sources of PD and electrical noise that are simultaneously present in a measurement process. This way, once the sources are completely separated through clusters on 2D or 3D separation maps, the subsequent identification process is much easier, since it can be carried out either traditionally, through

the individual analysis of the PRPD associated with a certain cluster, or through complementary methods based on intelligent pattern recognition algorithms.

As summarized in Table 1, each technique uses mathematical procedures based on the temporal or spectral behaviour of the signals, this way it is possible to characterize the signals in different distinctive parameters that are directly represented in the separation maps to form the respective

clusters associated with the different sources captured. The techniques described in sections B, C, D, E, H, and I are an example of the above, using the characteristic parameters obtained through fixed formulas or mathematical methods to represent them directly on the map of separation. One of the main advantages of these techniques is that they can be easily applied to on-line monitoring systems, since the computational cost is low. However, the presence of high-bandwidth external noise (white noise), that significantly change the spectral and temporal content of the captured signals, can limit their separation capacity and, in many cases, signals associated with multiple sources could be classified in the same cluster.

Other techniques such as those described in sections A, F and G require the application of PCA or SSNN, in order to reduce the dimensionality of the characteristic parameters obtained, and thus be able to represent them more easily on 2D or 3D maps. This occurs since an important number of parameters or variables are extracted from each detected signal which, according to the technique, can be considered of great interest and therefore, a subsequent reduction process is necessary. The main problem with this type of separation techniques is the additional computational cost that is generated when applying the dimensionality reduction process, which could be critical when it comes to being implemented in real-time monitoring systems. Additionally, white noise can also affect the performance of this type of techniques, despite including more characteristic parameters of the signals in the processing.

Furthermore, some techniques require additional signal processing in order to obtain better results during separation. In this sense, the technique described in section C requires the application of filter tools based on the wavelet transform in order to minimize the noise sources coupled during the measurement process. The same is the case with the $I_{peak}QE$ clusters technique, which requires a low-pass filter to minimize the effect of signal oscillations when it comes to more precisely obtain the apparent load value of the PD pulse. Likewise, the SPCT described in section I requires an adjustment of $f_{1l}, f_{2l}, f_{1h}, f_{2h},$ and $f_t,$ which can be done at the beginning or during the measurement, this way the best intervals can be established where the separation of the clusters is more evident. An advantage of applying this pre-processing on each captured signal is that external noise sources that are normally present during the measurement can be effectively mitigated. However, as in previous techniques, the computational cost could limit the use of these techniques in on-line monitoring systems. Additionally, if the preprocessing is not carried out correctly, the temporal and spectral behavior of the PD signals may change, which could be a problem for the subsequent identification process.

Finally, for any of these techniques, once the clusters have been established in the separation maps it is very common to use automatic cluster search methods such as DBSCAN, SSNN, FMC, FML, GMM and k-means (sections A, B, E, F, G and I). These methods allow to automatically search the different clusters with their respective PRPD. However, the methods are not always used since the selection can be made manually in the separation map, without affecting the result of the clustering technique.

## REFERENCES

[1] Y. Liao, H. Liu, J. Yuan, Y. Xu, W. Zhou, and C. Zhou, "A holistic approach to risk-based maintenance scheduling for HV cables," *IEEE Access*, vol. 7, pp. 118975–118985, 2019.

[2] P. Gill, *Electrical Power Equipment Maintenance and Testing*. New York, NY, USA: Marcel Dekker, 1998.

[3] T. Tanaka, "Aging of polymeric and composite insulating materials. Aspects of interfacial performance in aging," *IEEE Trans. Dielectrics Elect. Insul.*, vol. 9, no. 5, pp. 704–716, Oct. 2002, doi: 10.1109/TDEI.2002.1038658.

[4] R. Billinton and R. N. Allan, *Reliability Evaluation of Engineering Systems*. New York, NY, USA: Plenum, 1992.

[5] *IEEE Guide for Partial Discharge Testing of Shielded Power Cable Systems in a Field Environment*, IEEE Power Engineering Society, New York, NY, USA, 2007.

[6] A. C. Gjaerde, "Multi-factor ageing models-origin and similarities," in *Proc. Conf. Electr. Insul. Dielectric Phenomena*, Virginia Beach, VA, USA, Oct. 1995, pp. 199–204.

[7] A. C. Gjaerde, "A phenomenological aging model for combined thermal and electrical stress," *IEEE Trans. Dielectrics Elect. Insul.*, vol. 4, no. 6, pp. 674–680, Dec. 1997.

[8] P. Morshuis, "Partial discharge mechanisms," Ph.D. dissertation, Dept. Elect. Eng., Delft Univ., Delft, The Netherlands, 1993.

[9] R. J. Van Brunt, "Stochastic properties of partial-discharge phenomena," *IEEE Trans. Elect. Insul.*, vol. 26, no. 5, pp. 902–948, Oct. 1991.

[10] E. Lemke, *Guide for partial discharge measurement in compliance to IEC 60270 Std*, CIGRE Tech. Brochure, no. 366, Standard WG D1.33, 2008.

[11] J. H. Mason, "The deterioration and breakdown of dielectrics resulting from internal discharges," *Proc. IEE I, Gen.*, vol. 98, no. 109, pp. 44–59, 1951.

[12] L. Wang, A. Cavallini, G. C. Montanari, and L. Testa, "Evolution of pd patterns in polyethylene insulation cavities under AC voltage," *IEEE Trans. Dielectrics Electr. Insul.*, vol. 19, no. 2, pp. 533–542, Apr. 2012.

[13] G. C. Montanari and G. Mazzanti, "Ageing of polymeric insulating materials and insulation system design," *Polym. Int.*, vol. 51, no. 11, pp. 1151–1158, Nov. 2002.

[14] F.H. Kreuger, *Partial Discharge Detection in High-Voltage Equipment*. London, U.K.: Butterworths, 1989.

[15] P. Morshuis, "Degradation of solid dielectrics due to internal partial discharge: Some thoughts on progress made and where to go now," *IEEE Trans. Dielectrics Elect. Insul.*, 2005, vol. 12, no. 5, pp. 905–913, Oct. 2005.

[16] CIGRE Working Group 21.03, *Recognition of Discharges*, CIGRE Publication, Paris, France, 1969, pp. 61–98.

[17] L. Niemeyer, "A generalized approach to partial discharge modeling," *IEEE Trans. Dielectrics Electr. Insul.*, vol. 2, no. 4, pp. 510–528, Aug. 1995.

[18] F. H. Kreuger, E. Gulski, and A. Krivda, "Classification of partial discharges," *IEEE Trans. Electr. Insul.*, vol. 28, no. 6, pp. 917–931, Dec. 1993.

[19] G. Stone, "A perspective on online partial discharge monitoring for assessment of the condition of rotating machine stator winding insulation," *IEEE Elect. Insul. Mag.*, vol. 28, no. 5, pp. 8–13, Sep. 2012.

[20] C. Hudon and M. Belec, "Partial discharge signal interpretation for generator diagnostics," *IEEE Trans. Dielectrics Electr. Insul.*, vol. 12, no. 2, pp. 297–319, Apr. 2005.

[21] A. Cavallini, G. C. Montanari, F. Puletti, and A. Contin, "A new methodology for the identification of PD in electrical apparatus: Properties and applications," *IEEE Trans. Dielectrics Electr. Insul.*, vol. 12, no. 2, pp. 203–215, Apr. 2005.

[22] A. Cavallini, G. C. Montanari, A. Contin, and F. Pulletti, "A new approach to the diagnosis of solid insulation systems based on PD signal inference," *IEEE Elect. Insul. Mag.*, vol. 19, no. 2, pp. 23–30, Mar. 2003.

[23] G. J. Paoletti and A. Golubev, "Partial discharge theory and technologies related to medium-voltage electrical equipment," *IEEE Trans. Ind. Appl.*, vol. 37, no. 1, pp. 90–103, Jan./Feb. 2001.

[24] *High Voltage Test Techniques. Partial Discharge Measurements*, IEC, document 60270, 3 ed., 2000.

[25] *Rotating Electrical Machines–Part 27-2: Online Partial Discharge Measurements on the Stator Winding Insulation of Rotating Electrical Machines*, IEC, document TS 60034-27-2, 2012.

[26] G. Robles, E. Parrado-Hernández, J. Ardila-Rey, and J. M. Martínez-Tarifa, "Multiple partial discharge source discrimination with multiclass support vector machines," *Expert Syst. Appl.*, vol. 55, pp. 417–428, Aug. 2016.

[27] E. Parrado-Hernández, G. Robles, J. Ardila-Rey, and J. Martínez-Tarifa, "Robust condition assessment of electrical equipment with one class support vector machines based on the measurement of partial discharges," *Energies*, vol. 11, no. 3, p. 486, Feb. 2018.

[28] L. Hao, P. Lewin, J. Hunter, D. Swaffield, A. Contin, C. Walton, and M. Michel, "Discrimination of multiple PD sources using wavelet decomposition and principal component analysis," *IEEE Trans. Dielectrics Electr. Insul.*, vol. 18, no. 5, pp. 1702–1711, Oct. 2011.

[29] A. Cavallini, A. Contin, G. C. Montanari, and F. Puletti, "Advanced PD inference in on-field measurements. I. Noise rejection," *IEEE Trans. Dielectrics Elect. Insul.*, vol. 10, no. 2, pp. 216–224, Apr. 2003.

[30] F. Alvarez, F. Garnacho, A. Khamlichi, and J. Ortego, "Classification of partial discharge sources by the characterization of the pulses waveform," in *Proc. IEEE Int. Conf. Dielectrics (ICD)*, Jul. 2016, pp. 514–519.

[31] F. Alvarez, F. Garnacho, J. Ortego, and M. A. Sanchez-Uran, "A clustering technique for partial discharge and noise sources identification in power cables by means of waveform parameters," *IEEE Trans. Dielectrics Elect. Insul.*, vol. 23, no. 1, pp. 469–481, Feb. 2016.

[32] A. R. Mor, L. C. Castro Heredia, and F. A. Munoz, "New clustering techniques based on current peak value, charge and energy calculations for separation of partial discharge sources," *IEEE Trans. Dielectrics Electr. Insul.*, vol. 24, no. 1, pp. 340–348, Feb. 2017.

[33] M.-X. Zhu, J.-N. Zhang, Y. Li, Y.-H. Wei, J.-Y. Xue, J.-B. Deng, H.-B. Mu, G.-J. Zhang, and X.-J. Shao, "Partial discharge signals separation using cumulative energy function and mathematical morphology gradient," *IEEE Trans. Dielectrics Elect. Insul.*, vol. 23, no. 1, pp. 482–493, Feb. 2016.

[34] M.-X. Zhu, Q. Liu, J.-Y. Xue, J.-B. Deng, G.-J. Zhang, X.-J. Shao, W.-L. He, A.-X. Guo, and X.-W. Liu, "Self-adaptive separation of multiple partial discharge sources based on optimized feature extraction of cumulative energy function," *IEEE Trans. Dielectrics Electr. Insul.*, vol. 24, no. 1, pp. 246–258, Feb. 2017.

[35] M.-X. Zhu, Y.-B. Wang, D.-G. Chang, G.-J. Zhang, X.-J. Shao, J.-Y. Zhan, and J.-M. Chen, "Discrimination of three or more partial discharge sources by multi-step clustering of cumulative energy features," *IET Sci., Meas. Technol.*, vol. 13, no. 2, pp. 149–159, Mar. 2019.

[36] K. Firuzi, M. Vakilian, V. P. Darabad, B. T. Phung, and T. R. Blackburn, "A novel method for differentiating and clustering multiple partial discharge sources using s transform and bag of words feature," *IEEE Trans. Dielectrics Electr. Insul.*, vol. 24, no. 6, pp. 3694–3702, Dec. 2017.

[37] Y.-B. Wang, D.-G. Chang, S.-R. Qin, Y.-H. Fan, H.-B. Mu, and G.-J. Zhang, "Separating multi-source partial discharge signals using linear prediction analysis and isolation forest algorithm," *IEEE Trans. Instrum. Meas.*, vol. 69, no. 6, pp. 2734–2742, Jun. 2020.

[38] J. Zhang, G. R. Jones, J. W. Spencer, P. Jarman, I. J. Kemp, Z. Wang, P. L. Lewin, and R. K. Aggarwal, "Chromatic classification of RF signals produced by electrical discharges in HV transformers," *IEE Proc.-Gener., Transmiss. Distrib.*, vol. 152, no. 5, p. 629, 2005.

[39] J. A. Ardila-Rey, J. M. Martinez-Tarifa, M. Mejino, R. Albarracin, M. V. Rojas-Moreno, and G. Robles, "Chromatic classification of RF signals for partial discharges and noise characterization," in *Proc. IEEE Int. Conf. Solid Dielectrics (ICSD)*, Jun. 2013, pp. 67–70.

[40] J. Ardila-Rey, J. Montaña, B. de Castro, R. Schurch, J. Covolan Ulson, F. Muhammad-Sukki, and N. Bani, "A comparison of inductive sensors in the characterization of partial discharges and electrical noise using the chromatic technique," *Sensors*, vol. 18, no. 4, p. 1021, Mar. 2018, doi: 10.3390/s18041021.

[41] J. Ardila-Rey, J. Martinez-Tarifa, G. Robles, and M. Rojas-Moreno, "Partial discharge and noise separation by means of spectral-power clustering techniques," *IEEE Trans. Dielectrics Elect. Insul.*, vol. 20, no. 4, pp. 1436–1443, Aug. 2013.

[42] J. M. Martínez-Tarifa, J. A. Ardila-Rey, and G. Robles, "Partial discharge source recognition by means of clustering of spectral power ratios," *Meas. Sci. Technol.*, vol. 24, no. 12, Dec. 2013, Art. no. 125605.

[43] N. C. Sahoo, M. M. A. Salama, and R. Bartnikas, "Trends in partial discharge pattern classification: A survey," *IEEE Trans. Dielectrics Elect. Insul.*, vol. 12, no. 2, pp. 248–264, Apr. 2005.

[44] L. G. Weiss, "Wavelets and wideband correlation processing," *IEEE Signal Process. Mag.*, vol. 11, no. 1, pp. 13–32, Jan. 1994.

[45] L. Hao and P. Lewin, "Partial discharge source discrimination using a support vector machine," *IEEE Trans. Dielectrics Electr. Insul.*, vol. 17, no. 1, pp. 189–197, Feb. 2010.

[46] A. T. Carvalho, A. C. S. Lima, C. F. F. C. Cunha, and M. Petraglia, "Identification of partial discharges immersed in noise in large hydrogenerators based on improved wavelet selection methods," *Measurement*, vol. 75, pp. 122–133, Nov. 2015.

[47] S. Zhou, J. Tang, C. Pan, Y. Luo, and K. Yan, "Partial discharge signal denoising based on wavelet pair and block thresholding," *IEEE Access*, vol. 8, pp. 119688–119696, 2020.

[48] I. T. Jolliffe, *Principal Component Analysis*, 2nd ed. New York, NY, USA: Springer-Verlag, 2002.

[49] D. Dapeng, T. Letian, Q. Yong, W. Jiang, H. Chengjun, Z. Yi, and J. Xiuchen, "Experimental study and feature extraction on UHF partial discharge detection for typical model in air," in *Proc. Int. Conf. Condition Monitor. Diagnosis*, Beijing, China, Apr. 2008, pp. 1040–1043.

[50] J. A. Hunter, L. Hao, P. L. Lewin, D. Evagorou, A. Kyprianou, and G. E. Georghiou, "Comparison of two partial discharge classification methods," in *Proc. IEEE Int. Symp. Electr. Insul.*, San Diego, CA, USA, Jun. 2010, pp. 1–5.

[51] L. Kaufman and P. J. Rousseeuw, *Finding Groups in Data: An Introduction to Cluster Analysis*. New York, NY, USA: Wiley, 1990.

[52] M. Ester, H. P. Kriegel, J. Sander, and X. Xu, "A density-based algorithm for discovering clusters in large spatial databases with noise," in *Proc. Int. 2nd Conf. Knowl. Discovery Data Mining*, Portland, OR, USA, 1996, pp. 226–231.

[53] R. D. Nimmo, G. Callender, and P. L. Lewin, "Methods for wavelet-based autonomous discrimination of multiple partial discharge sources," *IEEE Trans. Dielectrics Elect. Insul.*, vol. 24, no. 2, pp. 1131–1140, Apr. 2017.

[54] A. Contin, A. Cavallini, G. C. Montanari, G. Pasini, and F. Puletti, "Digital detection and fuzzy classification of partial discharge signals," *IEEE Trans. Dielectrics Electr. Insul.*, vol. 9, no. 3, pp. 335–348, Jun. 2002.

[55] R. Bartnikas and J. P. Novak, "On the character of different forms of partial discharge and their related terminologies," *IEEE Trans. Elect. Insul.*, vol. 28, no. 6, pp. 956–968, Dec. 1993.

[56] P. Morshuis, "Assessment of dielectric degradation by ultrawide-band PD detection," *IEEE Trans. Dielectrics Electr. Insul.*, vol. 2, no. 5, pp. 744–760, 1995.

[57] A. Contin, A. Cavallini, G. C. Montanari, G. Pasini, and F. Puletti, "Artificial intelligence methodology for separation and classification of partial discharge signals," in *Proc. Annu. Rep. Conf. Electr. Insul. Dielectric Phenomena*, Victoria, BC, Canada, Oct. 2000, pp. 522–526.

[58] A. Rodrigo Mor, L. C. Castro Heredia, and F. A. Muñoz, "Effect of acquisition parameters on equivalent time and equivalent bandwidth algorithms for partial discharge clustering," *Int. J. Electr. Power Energy Syst.*, vol. 88, pp. 141–149, Jun. 2017.

[59] A. Hinneburg and D. A. Keim, "An efficient approach to clustering in large multimedia databases with noise," in *Proc. Int. Conf. Knowl. Discovery Data Mining*, 1998, pp. 58–65.

[60] M. Wu, H. Cao, J. Cao, H.-L. Nguyen, J. B. Gomes, and S. P. Krishnaswamy, "An overview of state-of-the-art partial discharge analysis techniques for condition monitoring," *IEEE Elect. Insul. Mag.*, vol. 31, no. 6, pp. 22–35, Nov. 2015.

[61] J. M. Martinez-Tarifa, J. A. Ardila-Rey, and G. Robles, "Automatic selection of frequency bands for the power ratios separation technique in partial discharge measurements: Part I, fundamentals and noise rejection in simple test objects," *IEEE Trans. Dielectrics Electr. Insul.*, vol. 22, no. 4, pp. 2284–2291, Aug. 2015.

[62] J. A. Ardila-Rey, J. M. Martinez-Tarifa, and G. Robles, "Automatic selection of frequency bands for the power ratios separation technique in partial discharge measurements: Part II, PD source recognition and applications," *IEEE Trans. Dielectrics Electr. Insul.*, vol. 22, no. 4, pp. 2293–2301, Aug. 2015.

[63] E. Montero, N. Medina, and J. Ardila-Rey, "An evaluation of meta-heuristic approaches for improve the separation of multiple partial discharge sources and electrical noise," in *Proc. IEEE 29th Int. Conf. Tools with Artif. Intell. (ICTAI)*, Boston, MA, USA, Nov. 2017, pp. 1166–1173.

[64] J. A. Ardila-Rey, E. Montero Ureta, and N. Medina Poblete, "Application of meta-heuristic approaches in the spectral power clustering technique (SPCT) to improve the separation of partial discharge and electrical noise sources," *IEEE Access*, vol. 7, pp. 110580–110593, 2019.

[65] G. Robles, J. Fresno, J. Martínez-Tarifa, J. Ardila-Rey, and E. Parrado-Hernández, "Partial discharge spectral characterization in HF, VHF and UHF bands using particle swarm optimization," *Sensors*, vol. 18, no. 3, p. 746, Mar. 2018.

[66] J. M. Fresno, J. A. Ardila-Rey, J. M. Martinez-Tarifa, and G. Robles, "Partial discharges and noise separation using spectral power ratios and genetic algorithms," *IEEE Trans. Dielectrics Electr. Insul.*, vol. 24, no. 1, pp. 31–38, Feb. 2017.

[67] R. Albarracin, "Separation of sources in radiofrequency measurements of partial discharges using time–power ratio maps," *ISA Trans.*, vol. 58, pp. 389–397, Sep. 2015, doi: 10.1016/j.isatra.2015.04.006.

**BRUNO ALBUQUERQUE DE CASTRO** (Member, IEEE) received the B.S., M.Sc., and Ph.D. degrees in electrical engineering from São Paulo State University, in 2019, with a period of a Sandwich Doctorate at the Aerospace Center, University of Surrey, U.K. He has published more than 40 technical journals, including IEEE and conference papers. His research interests include non-destructive inspection, electronic instrumentation, sensors, digital signal processing, acoustic emission, data acquisition, and intelligent systems. He was selected as the 2019 IEEE Transactions on Instrumentation and Measurement Outstanding Reviewer.

**JORGE ALFREDO ARDILA-REY** (Member, IEEE) was born in Santander, Colombia, in 1984. He received the B.Sc. degree in mechatronic engineering from the Universidad de Pamplona, Pamplona, Colombia, in 2007, the Specialist Officer degree in naval engineering from the Escuela Naval Almirante Padilla, Cartagena, Colombia, in 2008, and the M.Sc. and Ph.D. degrees in electrical engineering from the Universidad Carlos III de Madrid (UC3M), in 2012 and 2014, respectively. He was an Automatic Control Engineer of ARC Almirante Padilla, from 2008 to 2010. From 2010 to 2014, he has worked with the Department of Electrical Engineering and the High-Voltage Research and Test Laboratory (LINEALT), UC3M. He is currently working as a Professor with the Department of Electrical Engineering, Universidad Técnica Federico Santa María, Santiago, Chile. His research interests include data clustering, SHM systems, partial discharges, insulation systems diagnosis, and instrumentation and measurement techniques for high-frequency currents.

**ANDRÉ LUIZ ANDREOLI** (Member, IEEE) was born in Bauru, Brazil, in 1971. He received the degree in electrical engineering and the master's degree in industrial engineering from São Paulo State University (UNESP), Bauru, Brazil, in 1997 and 2005, respectively, and the Ph.D. degree in electrical engineering from the Escola de Engenharia de São Carlos, in 2011. He is currently a Professor with the Department of Electrical Engineering, Faculty of Engineering, UNESP. His research interests include industrial electronics, power quality, and electrical machines and drives.

**MATÍAS PATRICIO CERDA-LUNA** was born in Talca, Chile, in 1992. He received the B.Sc. degree in electrical engineering from the Universidad de Concepción, Concepción, Chile, in 2017. He was an Electrical Engineer with GORE Aysén, from 2018 to 2019. He currently works as a part-time Professor and a Researcher with the Department of Electrical Engineering, Universidad Técnica Federico Santa María, Santiago, Chile. His research interests include partial discharges, insulation systems diagnosis, and instrumentation and measurement techniques for high-frequency currents.

**FIRDAUS MUHAMMAD-SUKKI** (Member, IEEE) received the M.Eng. degree in electrical and electronic engineering from the Imperial College London, in 2006, and the master's and Ph.D. degrees from Glasgow Caledonian University, in 2009 and 2013, respectively. He is currently a Chartered Engineer, a member of the Institution of Engineering and Technology (IET), and an Associate of the City and Guilds, London (ACGI). He is currently a Lecturer with Robert Gordon University, U.K. His research interests include designing optical concentrator, which can be used in many applications, including creating a low-cost solar photovoltaic systems, illumination, heating and cooling of buildings, energy harvesting, desalination, medical devices, and waste water treatment. On top of that, he also carried out a number of non-technical researches, including market trend and financial analysis related to renewable technologies for countries such as Malaysia, Japan, Nigeria, Cameroon, and U.K. Prior to joining the academia, he was a communication engineer in Malaysia's largest telecommunication company.

**RODRIGO ANDRÉS ROZAS-VALDERRAMA** was born in Punta Arenas, Chile, in 1984. He received the B.Sc. degree in electrical engineering and the Electrical Engineer title and the master's degree in energy economics from the Universidad Técnica Federico Santa María, Santiago, Chile, in 2010 and 2016, respectively. From 2010 to 2018, he has worked as a Specialist Engineer in power system with Colbún S. A., the second biggest power generation company in Chile. He is currently a Professor with the Department of Electrical Engineering, Universidad Técnica Federico Santa María. His research interests include partial discharges, insulation systems diagnosis, power system stability, power plants, and instrumentation and measurement techniques.

• • •